

Toward the Chemogeography of Dissolved Organic Matter in the Global Ocean

Jianjun Wang,^{*,#} Ang Hu,[#] Yifan Cui,[#] Sarah Bercovici, Xiancai Lu, Jay Lennon, Janne Soininen, Yongqin Liu, and Nianzhi Jiao



Cite This: <https://doi.org/10.1021/acs.est.5c02477>



Read Online

ACCESS |



Metrics & More



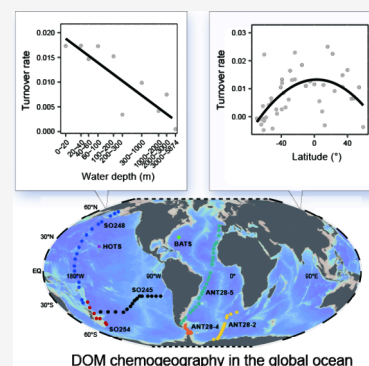
Article Recommendations



Supporting Information

ABSTRACT: Dissolved organic matter (DOM) comprises a diverse mixture of organic molecules, playing a critical role in marine biogeochemistry and Earth's climate. However, the ecological patterns and drivers of DOM composition at the global scale and their variation across compound classes remain unclear. Here we quantify the compositional turnover of over 800 DOM samples covering the surface waters to the deep across the global ocean, using distance–decay relationships based on an ultrahigh-resolution mass spectrometry data set. Molecular compositions become increasingly dissimilar to greater geographical distances in both horizontal and vertical dimensions. The observed turnover rates, consistent across biochemically labile and recalcitrant compound classes, progressively decrease toward the deep ocean and high latitudes, indicating a trend of chemohomogenization. The geographical distribution is jointly influenced by horizontal spatial distance, water depth, and physicochemical environments, which suggests that both stochastic and deterministic processes shape the DOM composition homogenization, effectively acting as a “carbon homogenizer”. This study unravels geographical patterns of DOM compositional turnover in the global ocean from an ecological perspective, deepening understanding of the forthcoming biogeochemical changes under global warming.

KEYWORDS: chemical ecology, chemogeography, dissolved organic matter, organic molecules, turnover rate, global ocean, geographical distribution, compound classes



DOM chemogeography in the global ocean

INTRODUCTION

Dissolved organic matter (DOM) in the ocean represents one of the largest carbon reservoirs on Earth, containing approximately 660 petagrams of carbon.¹ DOM consists of a highly diverse mixture of organic molecules, surpassing even the diversity of organisms, and plays a critical role in shaping biogeochemical cycles and influencing Earth's climate.^{2–4} However, our understanding of how the identities and abundances of individual organic molecules shift across spatiotemporal scales and how these shifts interact to drive ecological processes remains limited. This could be enhanced by testing the generality of existing conceptual frameworks and ecological theories of chemical systems. To address this gap, we introduce a novel, conceptual framework “chemogeography”, defined as the geographical patterns of organic molecules and the underlying driving factors. This is analogous to one of the central goals in ecology, that is, to understand the composition, diversity, and distribution of biological entities across temporal and spatial scales, and the underlying factors, mechanisms, and processes.⁵ The framework is critical for predicting DOM chemodiversity and understanding the persistence of carbon storage, especially in the context of anthropogenic global changes, such as climate warming.^{6–9}

DOM has shown spatial shifts in molecular composition across geographical gradients, such as latitude and depth, in

both marine and terrestrial environments.^{10–15} While such spatial shifts have been studied primarily in terms of chemodiversity and molecular traits,^{10,16,17} the quantitative changes in molecular compositions, specifically compositional turnover along spatial and temporal gradients, have rarely been systematically investigated across geographical scales. This turnover can be illuminated through the lens of ecological theory, such as the distance–decay relationship, which has been widely studied for plants, animals, and microbes.^{18–20} The distance–decay relationship describes how the similarity in species composition between two communities decreases with the geographical distance separating them and could help reveal the forces driving community turnover, such as environmental heterogeneity and dispersal limitation.^{18–20} However, such geographical analyses, including the distance–decay relationship, have only rarely, if ever, been used to study DOM. Therefore, quantitative answers remain elusive for key questions such as How does the rate of compositional

Received: February 21, 2025

Revised: October 6, 2025

Accepted: October 7, 2025

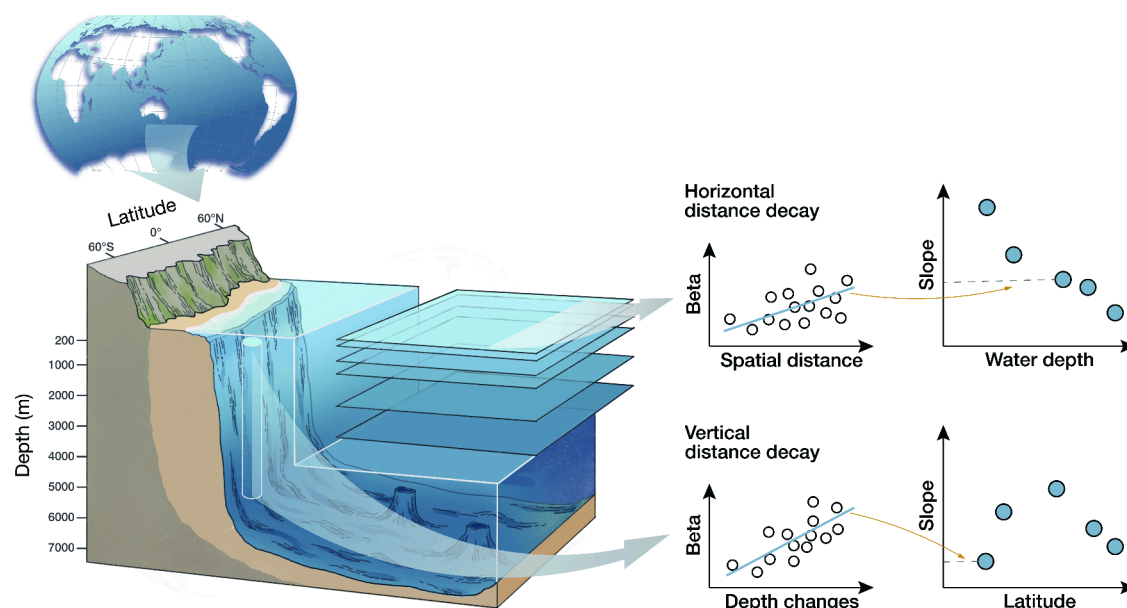


Figure 1. Conceptual illustration of compositional turnover rates of dissolved organic matter (DOM) across geographical gradients in the global ocean. We quantified DOM compositional turnover in two dimensions: horizontal (i.e., spatial) and vertical (i.e., depth-related). Turnover rates were calculated using distance–decay relationships, which represent linear regressions between the Bray–Curtis dissimilarity of pairwise DOM assemblages (i.e., beta diversity) and their corresponding spatial or depth distances. The resulting turnover rates, indicated by the slopes of the distance–decay relationships, were then plotted as functions of water depth (for horizontal turnover) and latitude (for vertical turnover) to reveal the global-scale geographical patterns in DOM compositional dynamics.

turnover vary across geographical gradients of the global ocean, and is it specific to, or influenced by, different biochemically defined compound classes of DOM?

Here, we used a global ocean molecular data set^{21–23} to examine the spatial and depth-related compositional turnover of DOM, reflecting horizontal and vertical variations, respectively (Figure 1). This DOM data set, measured with ultrahigh-resolution Fourier transform ion cyclotron resonance mass spectrometry (FT-ICR MS), comprises over 800 samples at 124 stations from the entire water column across a 5,800 m depth gradient in the Atlantic, Southern, and Pacific Oceans (Figure S1).²¹ Spatial and depth-related compositional turnover was assessed using distance–decay relationships, based on linear regressions between the Bray–Curtis dissimilarity of pairwise DOM assemblages and their respective spatial (i.e., horizontal) and depth (i.e., vertical) distances. The slope of each linear regression was used to quantify the rate of compositional turnover per unit distance, where a steeper slope indicates a faster decay of compositional similarity with increasing distance.^{18,19} We further assessed the spatial and depth-related turnover for subsets of samples grouped by the water depth and location of the sampling station. For spatial turnover, ten subsets of samples were organized by their water depths (hereafter “depth groups”). For depth-related turnover, 45 subsets of samples were organized by their stations, with each station containing over seven water depths (hereafter “station groups”). We finally examined the compositional turnover separately for each of the five DOM compound classes, classified based on van Krevelen diagrams²⁴ and aromaticity index^{25,26} (see Materials and Methods).

■ MATERIALS AND METHODS

Data Collection. We included a global ocean data set of dissolved organic matter (DOM) composition and environmental variables for examining the chemogeography of DOM

in the global ocean. This data set, which is available from previous literature,^{21–23} was generated by the Research Group for Marine Geochemistry at the Institute for Chemistry and Biology of the Marine Environment (Carl von Ossietzky University Oldenburg, Germany). Details of sample collection, DOM extraction, and FT-ICR MS analysis of DOM composition are provided in previous literature^{21,23,27} and briefly described as follows. The samples were obtained from 124 stations, covering the entire water column across depths from 5 to 5,874 m during six cruises in the Atlantic, Southern, and Pacific Oceans (Figure S1). The cruises spanned latitudes from 70.5° S to 43° N in the Atlantic and Southern Oceans and from 52° S to 59° N in the Pacific Ocean, including three *R.V. Polarstern* cruises ANT-XXVIII/2, ANT-XXVIII/4, and ANT-XXVIII/5 (Dec 2011 to May 2012) for the Atlantic and Southern Oceans, and three *R.V. Sonne* cruises SO245 (December 2015 to January 2016), SO248 (May 2016) and SO254 (January and February 2017) for the Pacific Ocean (Figure S1). All samples were collected from a rosette of Niskin samplers equipped with sensors for measuring environmental variables, such as water temperature and salinity.

DOM was solid-phase extracted (SPE) from water samples and measured on a solariX XR Fourier-transform ion cyclotron resonance mass spectrometer (FT-ICR MS) with a 15 T superconducting magnet (Bruker Daltonik GmbH, Bremen, Germany), as described previously.^{23,28} Briefly, 4 L of seawater was filtered through precombusted (400 °C, 4 h) 0.7- μ m glass fiber filters (GF/F, Whatman, United Kingdom), and the filtered water was acidified to pH 2 using 25% HCl and further extracted using 1 g PPL cartridges (Agilent Technologies). Cartridges were rinsed with pH 2 ultrapure water and dried with N₂ gas. The DOM was then eluted with 6 mL of methanol (HPLC-MS grade) into precombusted amber glass vials and immediately stored at –20 °C until FT-ICR MS analysis. The SPE-DOC concentrations were analyzed on a

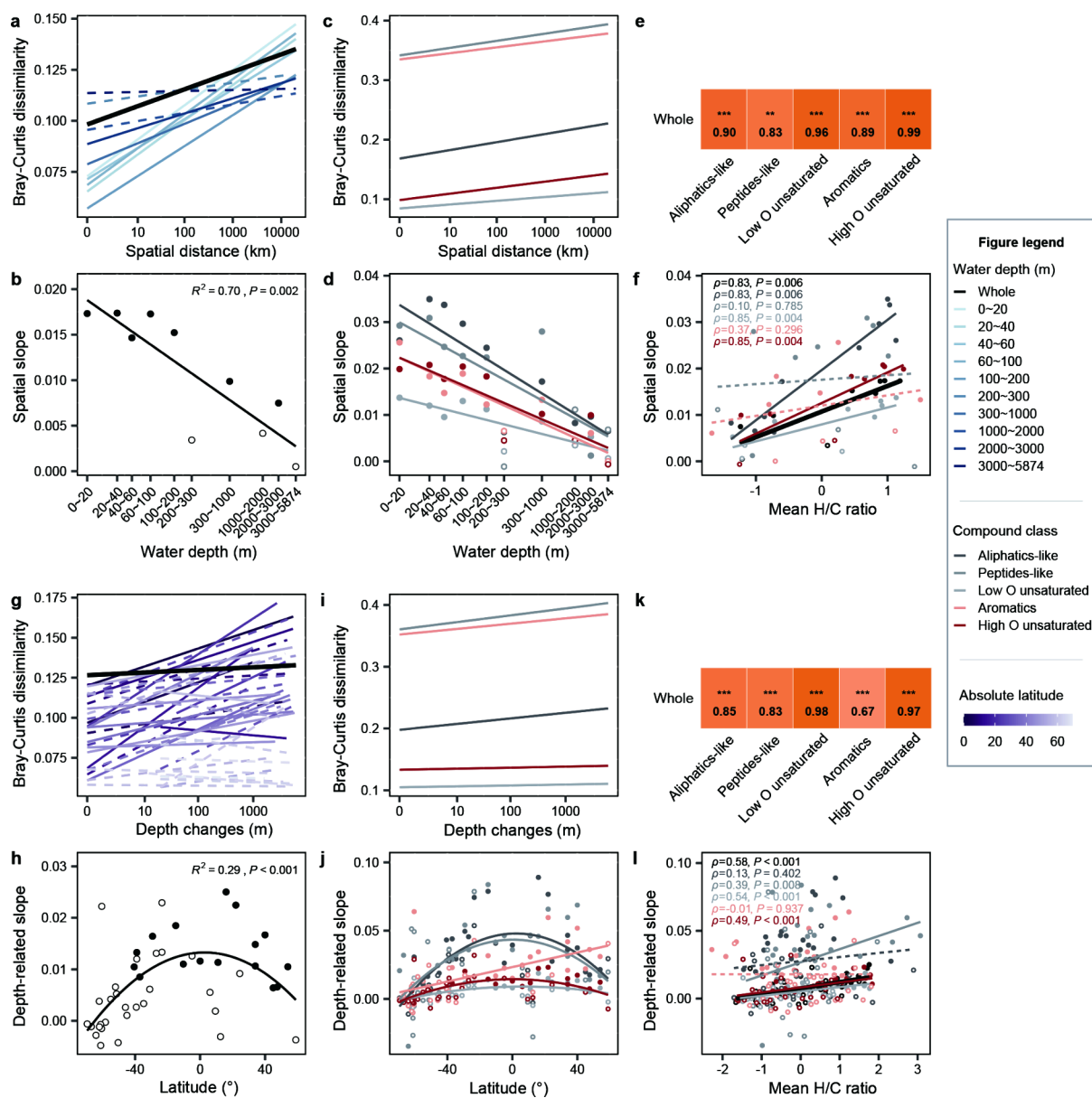


Figure 2. Geographical patterns of compositional turnover rates of dissolved organic matter (DOM) in the global ocean. The distance–decay relationships between Bray–Curtis dissimilarities of DOM composition and (a) spatial (i.e., horizontal) or (g) depth (i.e., vertical) distances are shown for the whole DOM assemblages (black line) and different sample groups. Ten depth groups (blue lines; a) and 45 station groups (purple lines; g) are defined in the [Materials and Methods](#). Statistical significance of the linear model is indicated by solid (statistically significant, ranked Mantel test, 9,999 permutations, $P \leq 0.05$) or dashed (statistically nonsignificant, $P > 0.05$) lines. We further plotted the spatial and depth-related compositional turnover rates, as indicated by the slope of the distance–decay relationship, against (b) the water depth and (h) the latitudes. Statistical significance of linear and quadratic model fits with one-sided F-statistics is indicated by solid ($P \leq 0.05$) lines. The (c) spatial- and (i) depth-related distance–decay relationships are also shown for each compound class (colored lines), and their slopes are plotted against (d) water depth and (j) latitudes. The line colors from gray to red represent the compound classes with decreasing H/C ratios. For better visualization, we omitted the data points in (a, c, g, i), but detailed scatter plots and statistics are shown in [Figures S2–S3, S7–S8](#). A heat map shows the Spearman's correlation coefficients ($***P < 0.001$, $**P < 0.01$) between the slopes of (e) spatial or (k) depth-related distance–decay relationship for the whole DOM assemblages and each compound class. The relationships between the slopes of (f) spatial or (l) depth-related distance–decay relationship and the H/C ratios of molecules are shown for the whole DOM assemblages (black line) and each compound class (colored lines).

Shimadzu TOC-VPCH total organic carbon analyzer. The mean (\pm SD) carbon-based extraction efficiency was $53 \pm 9\%$. Detailed methods for DOM extraction and extraction efficiency have been described previously.^{16,23} For FT-ICR MS analysis, the extracts were mixed with methanol and ultrapure water (MS grade, 1:1 v/v) to a final carbon concentration of $2.5 \text{ mg of C L}^{-1}$ immediately preceding FT-ICR MS analysis. For analysis validation, an in-house DOM

reference sample, collected at the Natural Energy Laboratory of Hawaii Authority in 2009,²⁹ was measured regularly. FT-ICR-MS measurements were conducted in electrospray ionization (ESI) negative ion mode, and putative chemical formulas were assigned following the same method described in Bercovici et al., (2022).²⁷

In total, 6,114 peaks had formula assignments for 821 samples, and these formulas were referred to as “molecules”

throughout the manuscript. The relative abundance (or intensity) of molecules was calculated by normalizing the signal intensity of each peak to the sum of all assigned intensities within each sample.³⁰ These molecules were categorized into seven compound classes based on van Krevelen diagrams²⁴ and modified aromaticity index (AI_{mod}).^{25,26} The compound classes were defined as follows: low O unsaturated ($AI_{\text{mod}} < 0.5$, $H/C < 1.5$, $O/C < 0.5$), high O unsaturated ($AI_{\text{mod}} < 0.5$, $H/C < 1.5$, $O/C = 0.5-0.9$), aliphatic-like ($H/C = 1.5-2.0$, $O/C < 0.9$, $N = 0$), peptide-like ($H/C = 1.5-2.0$, $O/C < 0.9$, $N > 0$), sugar-like ($H/C > 2.0$ or $O/C \geq 0.9$), aromatics ($AI_{\text{mod}} = 0.5-0.67$), and condensed aromatics ($AI_{\text{mod}} \geq 0.67$). It should be noted that compounds identified as “aliphatic-like”, “peptide-like”, and “sugar-like” have the molecular formulas of aliphatics, peptides, and sugars, but their actual structure may differ.²⁶

Statistical Analyses. To examine variation in the DOM composition across geographical gradients, i.e. compositional turnover, we used a distance–decay analysis where compositional dissimilarity is related to geographical distance among samples.^{18,19} DOM compositional dissimilarity was calculated using the Bray–Curtis dissimilarity index based on normalized peak intensities between pairwise samples.³⁰ We assessed spatial and depth-related compositional turnover through linear regressions between the Bray–Curtis dissimilarity of pairwise DOM assemblages and their respective spatial (i.e., horizontal) and depth (i.e., vertical) distances (expressed as logarithm). Significance was determined using Mantel tests (Spearman’s rank correlation) with 9,999 permutations.^{31,32} Spatial distance among samples was calculated as the great-circle distance on a sphere, based on their longitudes and latitudes.³³ Depth distance between pairwise samples was calculated as Euclidean distances based on water depth. The rate of compositional turnover was measured as the slope of the distance–decay relationship and subsequently plotted as functions of water depth (for horizontal turnover) and latitude (for vertical turnover) in order to reveal the global-scale geographical patterns in DOM compositional dynamics.

Additionally, we assessed spatial and depth-related turnover for subsets of samples grouped by water depth and location of the sampling station. For spatial turnover, ten subsets of samples were organized by water depth (hereafter “depth groups”), namely, 0–20, 20–40, 40–60, 60–100, 100–200, 200–300, 300–1,000, 1,000–2,000, 2,000–3,000, and >3,000 m. For depth-related turnover, 45 subsets of samples were organized by station, with each station containing more than seven water depths (hereafter “station groups”). To evaluate whether DOM compound classes exhibited compositional turnover across geographical gradients, we separately assessed the spatial and depth-related distance–decay relationships for each of the five DOM compound classes. The rate of compositional turnover was measured as the slope of the distance–decay relationship, and Spearman’s rank correlation was used to compare differences in turnover rates among DOM compound classes.

To confirm the results of spatial (i.e., horizontal) compositional turnover (Figures 1a–f, S2, S3), we considered different depths at each station as representing a single DOM assemblage. We calculated the average relative abundance of molecules across all depths or within each depth group and then performed the same analyses as described above. Consistent patterns were observed in the distance–decay

relationships and compositional turnover rates with increasing depths, as shown in Figures S4 and S5.

We further tested whether environmental distance could explain the Bray–Curtis dissimilarity of DOM using the Mantel test.³² Environmental distance was calculated as Euclidean distance based on standardized (*z*-scored) environmental variables, including water temperature, salinity, and SPE-DOC. The environmental influence was quantified as the Mantel statistic using a Spearman’s rank correlation between entries of two dissimilarity matrices. The significance of the Mantel statistic was tested by 9,999 permutations. To investigate whether environmental influences vary along the gradients of water depth and latitude, we analyzed the relationships between the Bray–Curtis dissimilarity of DOM and environmental distance for different depth groups and station groups.

Finally, we disentangled the pure and interactive effects of three driver categories—namely, space (i.e., horizontal distance), water depth, and environmental conditions—on the compositional dissimilarity of DOM using variation partitioning analysis (VPA).³⁴ The ‘space’ category was derived from principal coordinates of neighbor matrices (PCNM),³⁵ which quantify spatial trends across a range of scales based on eigenvalue decomposition of a truncated matrix of geographic distances among sampling sites, as determined on an ellipsoid map using R package *geosphere* V1.5–18.³³ The ‘environment’ category included water temperature, salinity, and SPE-DOC. We independently selected explanatory variables for the three driver categories for regression analyses by forward selection with Akaike information criterion (AIC)³⁶ prior to VPA analysis. VPA was performed for the whole DOM assemblages and for subsets of molecules within each of the five DOM compound classes with R package *vegan* V2.4.6.³¹

RESULTS AND DISCUSSION

The overall DOM assemblages exhibited compositions very similar across the oceans. Their Bray–Curtis dissimilarities ranged from 0.04 to 0.37, with a global mean (\pm SD) of 0.13 ± 0.004 (Figures 2a, S2). These observed dissimilarities were notably much lower than the documented values of respective DOM assemblages for lakes (0.08–0.46)³⁷ and rivers (0.04–0.92),³⁸ highlighting the high compositional similarity of marine DOM. For example, a study of the North Atlantic Ocean between 24° N and 68° N found a 96% similarity in DOM molecular composition.¹⁴ Such consistently low compositional variation among oceanic samples, compared with freshwater systems, is likely driven by prolonged microbial reworking or common synthetic pathways, which promote convergence toward a universal molecular pool.^{2,12} This pattern is consistent with the observations along the land-ocean continuum, where DOM composition becomes increasingly similar from terrestrial to marine environments as microbes transform plant-derived compounds, leaving DOM increasingly dominated by a shared set of recalcitrant, difficult-to-degrade molecules.¹²

Nevertheless, DOM assemblages across the global ocean showed a significant spatial distance–decay relationship; that is, compositional dissimilarities significantly increased with horizontal spatial distance (Figures 2a, S2). This relationship was also significant within 7 out of 10 depth groups, most of which occurred at shallow depths of <200 m ($P \leq 0.05$; Figures 2a, S2). Interestingly, the spatial compositional turnover rates, determined by the slope of the distance–

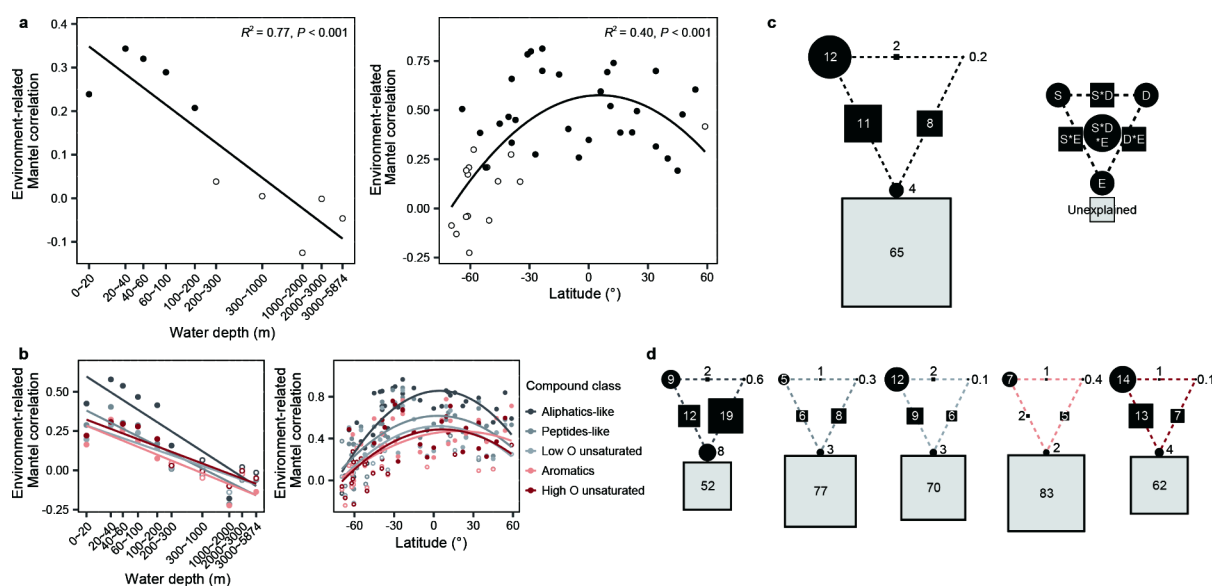


Figure 3. Relative importance of space (i.e., horizontal distance), water depth, and environmental conditions in explaining dissolved organic matter (DOM) composition in the global ocean. (a, b) Environmental constraints on DOM assemblages are plotted against water depth (left panels) and latitudes (right panels). The environmental constraints were assessed using Mantel tests, based on the Spearman's correlation between Bray–Curtis dissimilarities of DOM composition and environmental distances for (a) the whole DOM assemblages (black line) and (b) each compound class (colored lines). The line colors from gray to red represent the compound classes with decreasing H/C ratios. (c, d) Variance partitioning analysis showing the relative importance of space, water depth, and environmental conditions in explaining DOM composition for (c) the whole DOM assemblages (black triangle) and (d) each compound class (colored triangles). The numbers indicate the variance explained (%) by space (S), water depth (D), and environmental conditions (E).

decay relationship, decreased toward the deep ocean, indicating a trend of chemohomogenization in the deep ocean. Specifically, the spatial turnover rates, ranging from 0.001 to 0.017 per log(km) of horizontal spatial distance, showed a significantly inverse relationship with water depth, with an R^2 of 0.70 ($P < 0.001$; Figure 2b). This depth-related convergence was primarily associated with significantly decreasing molecular evenness toward deep waters ($P < 0.05$), rather than changes in the number of molecules ($P > 0.05$; Figure S6). This pattern suggests that compositional homogenization is driven by shifts in the relative abundance of molecules—where recalcitrant compounds increasingly dominate and labile molecules become rare, rather than by the outright loss or gain of individual molecules.

Our results provide the first quantitative assessment of a depth-dependent decrease in spatial turnover rates, offering global-scale evidence for a progressive homogenization of DOM molecular composition with water depth. Previous studies have documented depth- and latitude-dependent DOM variations at regional scales or based on several sample points,^{2,12,14} but a global, systematic assessment of spatial molecular turnover has been lacking. This “chemohomogenization” likely reflects a greater proportion of shared DOM molecules along the degradation cascades, such as from the surface and to the deep ocean.^{2,12,16} This pattern was supported by multiple lines of evidence of optical analyses of DOM. The optical properties, such as the absorption coefficient at 375 nm, the spectral slope between 300 and 650 nm, and the UV slope between 275 and 295 nm, show reduced spatial variations in deeper waters.³⁹ Likewise, the first two principal component axes derived from DOM indices such as fluorescence components and UV absorbance at 254 nm show decreasing variations with depth.⁴⁰

This phenomenon could be explained by a cascade of photodegradation together with the microbial-mediated transformation of DOM during its downward flux to the deep ocean.² These processes leave behind more similar residual components which are dominated by refractory compounds with common structural features, such as carboxylic-rich alicyclic moieties (CRAM) and material derived from linear terpenoids.^{41,42} In the deep ocean, conservative mixing of water masses further distributes these persistent molecules over broad spatial scales, reinforcing molecular convergence.¹⁴ Thus, both deterministic processes (e.g., biotic and abiotic drivers) and stochastic processes (e.g., dispersal processes mediated by physical transport)⁴³ jointly drive the chemohomogenization of DOM in the global ocean, effectively acting as a “carbon homogenizer”.

The observed chemohomogenization was consistently supported across various biochemically defined compound classes of DOM (Figure 2c,d). For instance, the molecular composition of each compound class became more dissimilar to increasing horizontal spatial distance ($P \leq 0.05$; Figures 2c, S3). Their spatial turnover rates also significantly decreased toward the deep ocean ($R^2 = 0.44$ to 0.80 ; $P < 0.001$; Figure 2d), with the rates being fastest for aliphatic and peptide-like compounds (mean slope = 0.020 and 0.018 per log(km) of horizontal spatial distance, respectively) and slowest for highly unsaturated compounds with low oxygen content (mean slope = 0.008 per log(km); Figure 2d). Notably, the homogenization trend for each compound class was highly similar to the whole DOM composition, with correlation coefficients of 0.83 to 0.99 ($P \leq 0.05$; Figure 2e).

Interestingly, a consistent chemohomogenization trend is also observed for recalcitrant compound classes, such as highly unsaturated compounds with high oxygen content (Figure 2d,e). These recalcitrant molecules are expected to be less

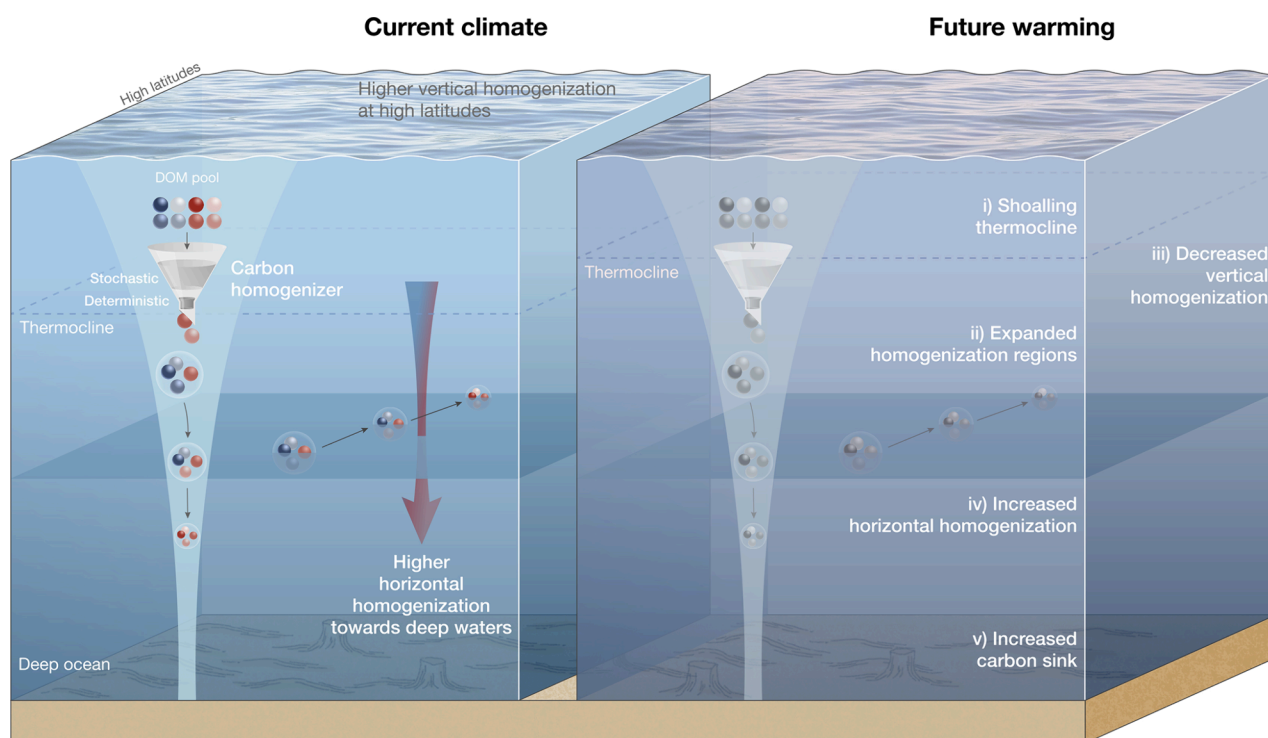


Figure 4. Chemohomogenization of DOM assemblages and its implications for understanding the long-term carbon cycle under future ocean warming. The left panel illustrates patterns of DOM compositional homogenization under current climate conditions, characterized by stronger vertical homogenization at high latitudes and greater horizontal homogenization in the deep ocean. As an example, we show horizontal homogenization: a local DOM assemblage (represented by a larger white circle) is formed from a diverse molecular pool (blue and red dots) through the joint effects of deterministic processes (e.g., biotic and abiotic drivers) and stochastic processes (e.g., physical transport) collectively acting as a “carbon homogenizer”. During the downward flux of DOM molecules, degradation and transformation processes leave behind residual components that are more compositionally similar and dominated by refractory compounds with shared structural features, resulting in increased homogenization of DOM across spatial scales toward the deep ocean. The right panel depicts hypothesized changes in DOM composition under future ocean warming. Specifically, warming is expected to enhance water-column stratification and shoal the thermocline, thereby expanding zones of horizontal molecular homogenization. Under these conditions, horizontal homogenization may intensify, whereas vertical homogenization, particularly at high latitudes, may weaken. These shifts imply that future warming may strengthen the role of the deep ocean as a long-term carbon sink.

likely reworked by microbial processes across geographical gradients in the same way as labile compound classes and have been selectively retained due to the high energetic costs required for their degradation.¹² We provided clear evidence that the chemohomogenization can be explained by molecular intrinsic traits of DOM, even for recalcitrant compound classes. That is, as the H/C ratios of molecules increased, there were elevated spatial turnover rates for the whole DOM composition, as well as for the compound classes such as aliphatic-like compounds, highly unsaturated compounds with low oxygen content, and highly unsaturated compounds with high oxygen content (Spearman $\rho = 0.83$ to 0.85 ; Figure 2f).

Furthermore, DOM assemblages also showed significant vertical (i.e., depth-related) distance–decay relationships, and their turnover rates exhibited hump-shaped patterns across latitudes within the sampled range (70.5° S to 59° N) (Figure 2g–j). Specifically, compositional Bray–Curtis dissimilarities significantly increased with depth distances across all samples and within 16 out of 45 station groups ($P < 0.05$; Figures 2g, S7). Similar to horizontal distance, we found consistently significant vertical distance–decay relationships across various compound classes of DOM (Figures 2i, S8). The depth-related turnover rates of the whole DOM composition, varying from -0.005 to 0.025 per $\log(m)$ of depth change, exhibited a significant latitudinal hump-shaped pattern, with the fastest

turnover occurring at the equator and the lowest turnover observed at higher latitudes ($R^2 = 0.29$; $P < 0.001$; Figure 2h). This hump-shaped pattern was also observed for most compound classes except for aromatics (Figure 2j), indicating more similar DOM assemblages associated with depth variations toward higher latitudes. Notably, the latitudinal patterns for each compound class were highly similar as for the whole DOM composition, with Spearman correlation coefficients of 0.67 to 0.98 ($P \leq 0.05$; Figure 2k). These latitudinal patterns were explained by molecular intrinsic traits of DOM, with depth-related turnover rates increasing with the H/C ratios of molecules (Spearman $\rho = 0.39$ to 0.58 ; Figure 2l). The faster vertical turnover at lower latitudes is likely because of the stronger stratification in these regions, where warm surface waters create a persistent density barrier that limits the vertical transport of DOM.⁴⁴ This physical isolation between surface and deep waters promotes greater compositional differentiation across depths, resulting in weaker vertical homogenization of the DOM compared to high-latitude regions.

We further found that the variation in DOM composition was shaped by environmental conditions including water temperature, salinity, and dissolved organic carbon, which interacted with space (i.e., horizontal distance) and water depth (Figure 3). For instance, the Bray–Curtis dissimilarity of

DOM composition increased significantly with environmental distance (Spearman $\rho = 0.29$), with temperature changes ($\rho = 0.34$) showing the strongest correlation, followed by dissolved organic carbon ($\rho = 0.18$) and salinity ($\rho = 0.11$) (Figure S9). This relationship was significant ($P \leq 0.05$) only at shallow depths of <200 m (Spearman $\rho = 0.21$ to 0.34 in Mantel test; Figure 3a), and across station groups, it held in 30 out of 45 cases, predominantly between latitudes 40 ° S and 50 ° N (Spearman $\rho = 0.19$ to 0.81 in Mantel test; Figure 3a).

Similar to geographical compositional turnover, the environmental constraints on the DOM assemblages showed predictable patterns along both depth and latitudinal gradients (Figure 3a). Specifically, the Spearman coefficients between compositional dissimilarity of the whole DOM assemblages and environmental distance showed a markedly decreased pattern over water depth ($R^2 = 0.77$; $P < 0.001$), and a hump-shaped pattern along the latitudinal gradient ($R^2 = 0.40$; $P < 0.001$; Figure 3a). These depth- and latitude-related patterns were consistently supported across the five compound classes, such as aliphatic-like, peptide-like, and highly unsaturated compounds with low oxygen content (Figure 3b). The geographical patterns of environmental constraints on the DOM assemblages were linked to the depth- and latitude-related shifts in the spatial (i.e., horizontal) and vertical variations of environmental factors themselves (Figure S10).

The above phenomenon indicates that the variation in DOM composition explained by environmental conditions was largely geographically structured. This is further evidenced by the joint effects of 0–13% between the environment and space and the joint effects of 5–19% between environment and depth for the whole DOM composition (Figure 3c) and the five compound classes (Figure 3d). Notably, the pure effects of space were much larger (5–14%) than that of the environment (2–8%) for the whole DOM composition and the five compound classes (Figure 3c,d). These results collectively indicate that, while environmental conditions deterministically shaped DOM assemblages, spatial factors alone accounted for a substantial proportion of the variation. Such pronounced pure spatial effects likely suggest a strong influence of dispersal limitation and/or unmeasured environmental variables¹⁸ on DOM molecular distribution. These effects may arise from restricted molecular movement over geographic distances despite the long-distance, long-term transport of molecules within and across oceans through ocean overturning,^{14,22} as well as from the low concentrations of molecules due to intrinsic recalcitrance or effective dilution.⁴⁵

The observed homogenization toward a stable DOM pool has important implications for understanding the long-term carbon cycle under future ocean warming (Figure 4). This compositional convergence may be particularly sensitive to environmental changes such as elevated temperatures, which are expected to enhance water-column stratification and shoal the thermocline.^{46,47} Under such conditions, enhanced stratification isolates deeper waters from surface influence, that is, elevated dispersal limitation of DOM molecules, allowing refractory dissolved organic carbon to gradually accumulate below the thermocline.⁴ Without effective physical connectivity to the surface, these intrinsically recalcitrant compounds are less likely to be transported upward and oxidized, favoring their longer-term preservation in the deep ocean.⁴ Notably, our findings show that deep-ocean regions currently exhibit greater horizontal homogenization in DOM composition, while high-latitude regions exhibit more

pronounced vertical homogenization. With future warming expected to enhance stratification particularly at high latitudes, horizontal homogenization may intensify, whereas vertical homogenization may weaken. Collectively, these changes could expand the zones of (horizontal) molecular homogenization under future warming and alter DOM persistence and the roles of the deep ocean as a carbon sink. Although the precise effect on the long-term carbon sink remains uncertain, recent evidence, including the potential contributions of photochemically transformed DOM to deep-ocean recalcitrant DOC over the past seven decades (1950–2020),⁴⁸ supports the possibility that warming-induced changes in homogenization may enhance the contribution of the deep ocean to long-term carbon sequestration.

In summary, our study presents the first quantification of the geographical compositional turnover patterns of DOM assemblages in the global ocean, both horizontally and vertically. The key finding is that DOM shows a remarkable chemohomogenization trend toward the deep ocean and higher latitudes, within the observed range (70.5° S to 59° N). We further demonstrate that the predictable patterns are highly similar for the whole DOM assemblages as well as for various biochemically defined compound classes. These findings underscore the importance of accounting for the geographically structured distribution of dissolved organic matter (jointly constrained by horizontal spatial distance, water depth, and physicochemical environments) in understanding its transformation and persistence in the ocean under global change. In future studies, we encourage the inclusion of data from additional ocean regions, such as polar and undersampled regions, and we expect that the generality of our main findings will be further validated. The quantified compositional turnover rates are comparable to those observed in other ocean habitats and ecosystems and may serve as benchmarks for future studies. With future ocean warming, horizontal homogenization may intensify, whereas vertical homogenization may weaken, potentially influencing its biogeochemical role in the ocean.

■ ASSOCIATED CONTENT

Data Availability Statement

The DOM and associated environmental data in the global ocean are available at PANGAEA Data Publisher (<https://doi.org/10.1594/PANGAEA.962747>).

SI Supporting Information

The Supporting Information is available free of charge at <https://pubs.acs.org/doi/10.1021/acs.est.5c02477>.

Additional information on the map of sampling sites, the distance–decay relationships between Bray–Curtis dissimilarities of DOM composition and horizontal spatial distance, the distance–decay relationships between Bray–Curtis dissimilarities of DOM composition for each compound class and horizontal spatial distance, the horizontal compositional turnover rates of DOM along the gradient of water depth, the distance–decay relationships between Bray–Curtis dissimilarities of DOM composition and horizontal spatial distance at the site level, the richness and evenness of DOM assemblages along the gradient of water depth, the distance–decay relationships between Bray–Curtis dissimilarities of DOM composition and depth changes, the distance–decay relationships between Bray–Curtis

dissimilarities of DOM composition for each compound class and depth changes, the relationships between Bray–Curtis dissimilarities of DOM composition and environmental distance, and the depth- and latitude-related shifts in the spatial (i.e., horizontal) and vertical variations (standard deviation; SD) of environmental factors (PDF)

AUTHOR INFORMATION

Corresponding Author

Jianjun Wang – State Key Laboratory of Lake and Watershed Science for Water Security, Nanjing Institute of Geography and Limnology, Chinese Academy of Sciences, Nanjing 211135, China; orcid.org/0000-0001-7039-7136; Email: jjwang@niglas.ac.cn

Authors

Ang Hu – State Key Laboratory of Lake and Watershed Science for Water Security, Nanjing Institute of Geography and Limnology, Chinese Academy of Sciences, Nanjing 211135, China; orcid.org/0000-0002-5755-2442

Yifan Cui – State Key Laboratory of Lake and Watershed Science for Water Security, Nanjing Institute of Geography and Limnology, Chinese Academy of Sciences, Nanjing 211135, China; orcid.org/0000-0003-2541-7737

Sarah Bercovici – Institute for Chemistry and Biology of the Marine Environment (ICBM), University of Oldenburg, Oldenburg 26129, Germany; National Oceanography Centre, Southampton SO14 3ZH Hampshire, United Kingdom; orcid.org/0000-0002-6877-9909

Xiancai Lu – State Key Laboratory for Mineral Deposits Research, School of Earth Sciences and Engineering, Nanjing University, Nanjing 210023, China; orcid.org/0000-0001-8977-2661

Jay Lennon – Department of Biology, Indiana University, Bloomington, Indiana 47405, United States

Janne Soinen – Department of Geosciences and Geography, University of Helsinki, Helsinki FIN-00014, Finland

Yongqin Liu – Center for the Pan-third Pole Environment, Lanzhou University, Lanzhou 730000, China

Nianzhi Jiao – Innovation Research Center for Carbon Neutralization, Fujian Key Laboratory of Marine Carbon Sequestration, Xiamen University, Xiamen 361000, China

Complete contact information is available at: <https://pubs.acs.org/10.1021/acs.est.5c02477>

Author Contributions

[#]JW, AH, and YC contributed equally to this paper.

Author Contributions

JW conceived the idea. SB provided the DOM and physiochemical data. YC, AH, and JW performed the statistical analyses. AH and JW wrote the first draft of the manuscript. AH and JW finished the manuscript with comments from JTL, JS, SB, XL, YL, and NJ. All authors contributed to the intellectual development of this study.

Notes

The authors declare no competing financial interest.

ACKNOWLEDGMENTS

We gratefully acknowledge the scientific party and crew of the cruises mentioned, and the group of Thorsten Dittmar for their kind support and data sharing, as detailed in previous reports

(e.g., Bercovici et al. *Environ. Sci. Technol.* **2023**, *57*, 21145–21155). This study was supported by the National Natural Science Foundation of China (42225708, 42377122, U24A20578, 92251304), the Basic Research Program of Jiangsu (BK20240111), the Global Ocean Negative Carbon Emissions (Global ONCE) Program, the Southern Marine Science and Engineering Guangdong Laboratory (Zhuhai) (SML2024SP022, SML2024SP002), the Key Laboratory of Lake and Watershed Science for Water Security (NKL2023-QN04), and the Science and Technology Planning Project of NIGLAS (NIGLAS2022GS09).

REFERENCES

- (1) Hansell, D.; Carlson, C.; Repeta, D.; Schlitzer, R. Dissolved Organic Matter in the Ocean: A Controversy Stimulates New Insights. *Oceanography* **2009**, *22* (4), 202–211.
- (2) Zark, M.; Dittmar, T. Universal molecular structures in natural dissolved organic matter. *Nat. Commun.* **2018**, *9* (1), 3178.
- (3) Dittmar, T.; Lennartz, S. T.; Buck-Wiese, H.; Hansell, D. A.; Santinelli, C.; Vanni, C.; Blasius, B.; Hehemann, J.-H. Enigmatic persistence of dissolved organic matter in the ocean. *Nature Reviews Earth & Environment* **2021**, *2*, 570–583.
- (4) Jiao, N.; Luo, T.; Chen, Q.; Zhao, Z.; Xiao, X.; Liu, J.; Jian, Z.; Xie, S.; Thomas, H.; Herndl, G. J.; Benner, R.; Gonsior, M.; Chen, F.; Cai, W.-J.; Robinson, C. The microbial carbon pump and climate change. *Nature Reviews Microbiology* **2024**, *22*, 408–419.
- (5) Brown, J. H.; Lomolino, M. V. *Biogeography*; Sinauer Associates Publishers, 1998.
- (6) Duarte, C. M. Global change and the future ocean: a grand challenge for marine sciences. *Frontiers in Marine Science* **2014**, *1*, 63. Specialty Grand Challenge.
- (7) Penn, J. L.; Deutsch, C. Avoiding ocean mass extinction from climate warming. *Science* **2022**, *376* (6592), 524–526.
- (8) Tanentzap, A. J.; Fonvielle, J. A. Chemodiversity in freshwater health. *Science* **2024**, *383* (6690), 1412–1414.
- (9) Hu, A.; Jang, K.-S.; Tanentzap, A. J.; Zhao, W.; Lennon, J. T.; Liu, J.; Li, M.; Stegen, J.; Choi, M.; Lu, Y.; Feng, X.; Wang, J. Thermal responses of dissolved organic matter under global change. *Nat. Commun.* **2024**, *15* (1), 576.
- (10) Hu, A.; Han, L.; Lu, X.; Zhang, G.; Wang, J. Global patterns and drivers of dissolved organic matter across Earth systems: Insights from H/C and O/C ratios. *Fundamental Research* **2025**, *5* (5), 2121–2132, DOI: [10.1016/j.fmre.2023.11.018](https://doi.org/10.1016/j.fmre.2023.11.018).
- (11) Roth, V.-N.; Lange, M.; Simon, C.; Hertkorn, N.; Bucher, S.; Goodall, T.; Griffiths, R. I.; Mellado-Vázquez, P. G.; Mommer, L.; Oram, N. J.; Weigelt, A.; Dittmar, T.; Gleixner, G. Persistence of dissolved organic matter explained by molecular changes during its passage through soil. *Nature Geoscience* **2019**, *12* (9), 755–761.
- (12) Freeman, E. C.; Emilson, E. J. S.; Dittmar, T.; Braga, L. P. P.; Emilson, C. E.; Goldhammer, T.; Martineau, C.; Singer, G.; Tanentzap, A. J. Universal microbial reworking of dissolved organic matter along environmental gradients. *Nat. Commun.* **2024**, *15* (1), 187.
- (13) Seidel, M.; Vemulapalli, S. P. B.; Mathieu, D.; Dittmar, T. Marine Dissolved Organic Matter Shares Thousands of Molecular Formulae Yet Differs Structurally across Major Water Masses. *Environ. Sci. Technol.* **2022**, *56* (6), 3758–3769.
- (14) Hansman, R. L.; Dittmar, T.; Herndl, G. J. Conservation of dissolved organic matter molecular composition during mixing of the deep water masses of the northeast Atlantic Ocean. *Marine Chemistry* **2015**, *177*, 288–297.
- (15) Han, L.; Hu, A.; Mzuka, H.; Chen, X.; Shen, J.; Wang, J. Molecular properties of dissolved organic matter across Earth systems: A meta-analysis. *Journal of Earth Science* **2025**, *36* (6), 1–15.
- (16) Mentges, A.; Feenders, C.; Seibt, M.; Blasius, B.; Dittmar, T. Functional Molecular Diversity of Marine Dissolved Organic Matter Is Reduced during Degradation. *Frontiers in Marine Science* **2017**, *4*, 194.

- (17) Hu, A.; Stegen, J.; Tanentzap, A. J.; Wang, J. The Emergence and Promise of Functional Biogeography of Organic Matter. *Global Change Biology* **2025**, *31* (8), No. e70435.
- (18) Wang, J.; Shen, J.; Wu, Y.; Tu, C.; Soininen, J.; Stegen, J. C.; He, J.; Liu, X.; Zhang, L.; Zhang, E. Phylogenetic beta diversity in bacterial assemblages across ecosystems: deterministic versus stochastic processes. *ISME J.* **2013**, *7* (7), 1310–1321.
- (19) Soininen, J.; McDonald, R.; Hillebrand, H. The distance decay of similarity in ecological communities. *Ecography* **2007**, *30* (1), 3–12.
- (20) Morlon, H.; Chuyong, G.; Condit, R.; Hubbell, S.; Kenfack, D.; Thomas, D.; Valencia, R.; Green, J. L. A general framework for the distance–decay of similarity in ecological communities. *Ecology Letters* **2008**, *11* (9), 904–917.
- (21) Bercovici, S.; Osterholz, H.; Wiemers, M.; Noriega-Ortega, B. E.; Dittmar, T.; Niggemann, J. Dissolved Organic Matter Molecular Composition Data and Supporting Metadata for Multiple Oceanographic Cruises with RV SONNE (SO254, SO245, SO248) and RV POLARSTERN (PS79). *Bermuda Atlantic Time-Series Study and Hawaii Ocean Time-Series*; PANGAEA, 2023, DOI: [10.1594/PANGAEA.962747](https://doi.org/10.1594/PANGAEA.962747).
- (22) Bercovici, S. K.; Dittmar, T.; Niggemann, J. Processes in the Surface Ocean Regulate Dissolved Organic Matter Distributions in the Deep. *Global Biogeochemical Cycles* **2023**, *37* (12), No. e2023GB007740.
- (23) Bercovici, S. K.; Wiemers, M.; Dittmar, T.; Niggemann, J. Disentangling Biological Transformations and Photodegradation Processes from Marine Dissolved Organic Matter Composition in the Global Ocean. *Environ. Sci. Technol.* **2023**, *57* (50), 21145–21155.
- (24) Kim, S.; Kramer, R. W.; Hatcher, P. G. Graphical Method for Analysis of Ultrahigh-Resolution Broadband Mass Spectra of Natural Organic Matter, the Van Krevelen Diagram. *Anal. Chem.* **2003**, *75* (20), 5336–5344.
- (25) Koch, B. P.; Dittmar, T. From mass to structure: an aromaticity index for high-resolution mass data of natural organic matter. *Rapid Commun. Mass Spectrom.* **2016**, *30* (1), 250–250.
- (26) Spencer, R. G. M.; Guo, W.; Raymond, P. A.; Dittmar, T.; Hood, E.; Fellman, J.; Stubbins, A. Source and biolability of ancient dissolved organic matter in glacier and lake ecosystems on the Tibetan Plateau. *Geochim. Cosmochim. Acta* **2014**, *142*, 64–74.
- (27) Bercovici, S. K.; Dittmar, T.; Niggemann, J. The detection of bacterial exometabolites in marine dissolved organic matter through ultrahigh-resolution mass spectrometry. *Limnology and Oceanography: Methods* **2022**, *20* (6), 350–360.
- (28) Dittmar, T.; Koch, B.; Hertkorn, N.; Kattner, G. A simple and efficient method for the solid-phase extraction of dissolved organic matter (SPE-DOM) from seawater. *Limnology and Oceanography: Methods* **2008**, *6* (6), 230–235.
- (29) Green, N. W.; Perdue, E. M.; Aiken, G. R.; Butler, K. D.; Chen, H.; Dittmar, T.; Niggemann, J.; Stubbins, A. An intercomparison of three methods for the large-scale isolation of oceanic dissolved organic matter. *Marine Chemistry* **2014**, *161*, 14–19.
- (30) Meng, F.; Hu, A.; Jang, K.; Wang, J. iDOM: Statistical analysis of dissolved organic matter characterized by high-resolution mass spectrometry. *mLife* **2025**, *4*, 319–331.
- (31) Oksanen, J.; Blanchet, F. G.; Kindt, R.; Legendre, P.; Minchin, P.; O'Hara, R. B.; Simpson, G.; Solymos, P.; Stevens, M. H. H.; Wagner, H. *vegan: Community Ecology Package*. CRAN R package, 2017.
- (32) Mantel, N. The Detection of Disease Clustering and a Generalized Regression Approach. *Cancer Res.* **1967**, *27* (2_Part_1), 209–220.
- (33) Hijmans, R. J.; Williams, E.; Vennes, C. Geosphere: spherical trigonometry. *R package version*, 2019, *1*, 10.
- (34) Borcard, D.; Legendre, P.; Drapeau, P. Partialling out the spatial component of ecological variation. *Ecology* **1992**, *73*, 1045–1055.
- (35) Borcard, D.; Legendre, P. All-scale spatial analysis of ecological data by means of principal coordinates of neighbour matrices. *Ecological Modelling* **2002**, *153* (1), 51–68.
- (36) Miller, J. K.; Farr, S. D. Bimultivariate redundancy: a comprehensive measure of interbattery relationship. *Multivariate Behavioral Research* **1971**, *6*, 313–324.
- (37) Kida, M.; Merder, J.; Fujitake, N.; Tanabe, Y.; Hayashi, K.; Kudoh, S.; Dittmar, T. Determinants of Microbial-Derived Dissolved Organic Matter Diversity in Antarctic Lakes. *Environ. Sci. Technol.* **2023**, *57* (13), 5464–5473.
- (38) Cui, Y.; Wen, S.; Stegen, J. C.; Hu, A.; Wang, J. Chemodiversity of riverine dissolved organic matter: Effects of local environments and watershed characteristics. *Water Res.* **2024**, *250*, No. 121054.
- (39) Stedmon, C. A.; Nelson, N. B. Chapter 10 - The Optical Properties of DOM in the Ocean. In *Biogeochemistry of Marine Dissolved Organic Matter*, Second ed.; Hansell, D. A., Carlson, C. A., Eds.; Academic Press, 2015; pp 481–508.
- (40) Lu, Y.; Edmonds, J. W.; Yamashita, Y.; Zhou, B.; Jaegge, A.; Baxley, M. Spatial variation in the origin and reactivity of dissolved organic matter in Oregon-Washington coastal waters. *Ocean Dynamics* **2015**, *65* (1), 17–32.
- (41) Hertkorn, N.; Benner, R.; Frommberger, M.; Schmitt-Kopplin, P.; Witt, M.; Kaiser, K.; Kettrup, A.; Hedges, J. I. Characterization of a major refractory component of marine dissolved organic matter. *Geochim. Cosmochim. Acta* **2006**, *70* (12), 2990–3010.
- (42) Lechtenfeld, O. J.; Kattner, G.; Flerus, R.; McCallister, S. L.; Schmitt-Kopplin, P.; Koch, B. P. Molecular transformation and degradation of refractory dissolved organic matter in the Atlantic and Southern Ocean. *Geochim. Cosmochim. Acta* **2014**, *126*, 321–337.
- (43) Hu, A.; Jang, K.-S.; Meng, F.; Stegen, J.; Tanentzap, A. J.; Choi, M.; Lennon, J. T.; Soininen, J.; Wang, J. Microbial and Environmental Processes Shape the Link between Organic Matter Functional Traits and Composition. *Environ. Sci. Technol.* **2022**, *56* (14), 10504–10516.
- (44) Sigman, D. M.; Jaccard, S. L.; Haug, G. H. Polar ocean stratification in a cold climate. *Nature* **2004**, *428* (6978), 59–63.
- (45) Arrieta, J. M.; Mayol, E.; Hansman, R. L.; Herndl, G. J.; Dittmar, T.; Duarte, C. M. Dilution limits dissolved organic carbon utilization in the deep ocean. *Science* **2015**, *348* (6232), 331–333.
- (46) Williams, B.; Grottole, A. G. Recent shoaling of the nutricline and thermocline in the western tropical Pacific. *Geophys. Res. Lett.* **2010**, *37* (22). DOI: [10.1029/2010GL044867](https://doi.org/10.1029/2010GL044867).
- (47) Holt, J.; Harle, J.; Wakelin, S.; Jardine, J.; Hopkins, J. Why Is Seasonal Density Stratification in Shelf Seas Expected to Increase Under Future Climate Change? *Geophys. Res. Lett.* **2022**, *49* (23), No. e2022GL100448.
- (48) Hu, A.; Cui, Y.; Bercovici, S.; Tanentzap, A. J.; Lennon, J. T.; Lin, X.; Yang, Y.; Liu, Y.; Osterholz, H.; Dong, H.; Lu, Y.; Jiao, N.; Wang, J. Photochemical processes drive thermal responses of dissolved organic matter in the dark ocean. *bioRxiv*, 2024, DOI: [10.1101/2024.09.06.611638](https://doi.org/10.1101/2024.09.06.611638).